Received: 27 June 2023 | Revised: 1 November 2023 | Accepted: 16 November 2023

DOI: 10.1002/eqe.4052

RESEARCH ARTICLE

WILEY

Equivalent static methods for seismic design of straight integral abutment bridges

Andrea Marchi | **Paolo Franchin**

Department of Structural and Geotechnical Engineering, Sapienza University of Rome, Rome, Italy

Correspondence
Andrea Marchi, Department of Structural and Geotechnical Engineering, Sapienza University of Rome, Rome, Italy.
Email: andrea.marchi@uniroma1.it

Funding information
Dipartimento della Protezione Civile, Presidenza del Consiglio dei Ministri

Abstract

Integral abutment bridges (IABs) are becoming the solution of choice in the low to mid-length ranges because of their low cost compared with traditional solutions and their good performance under seismic actions. The main drawback of these bridges is the need to consider soil-structure interaction to assess their performance, a problem that is more pronounced for actions implying horizontal deck movements, such as temperature or the specific focus of this paper, that is, seismic action. In IAB design, simplified models are often used, where soil-structure interaction is modeled by means of beams on non-linear Winkler springs for the evaluation of seismic behavior. This paper, starting from an existing non-linear dynamic model (NLDM) that describes IABs longitudinal seismic response, derives two equivalent static models: one non-linear and the other linear, for displacement- or force-based design respectively. A parametric study is carried out to assess the static models performance in terms of the main design internal actions versus the NLDM. Finally, the assessed model errors are discussed in the context of partial factors safety format.

KEYWORDS

displacement-based design, performance-based design, soil-structure interaction, simplified analysis, Winkler

1 | INTRODUCTION

Integral abutment bridges (IABs) are defined as single or multiple span bridges in which the deck is monolithically connected to the abutment walls. They are very popular due to their low initial and maintenance costs, partly due to the absence of bearings and joints.[1,2] Their development started in the 1960s in the United States of America and they were later adopted in the UK and Europe. In terms of seismic performance this type of bridges has exhibited, in the past, better response compared to traditional bridges: in particular, after the 1989 Loma Prieta and 1994 Northridge earthquakes in California, after the 2010–2011 Canterbury seismic sequence and 2013 Lake Grassmere earthquake in New Zealand and after the 2011 Tōhoku Earthquake in Japan.[3–5] Despite these advantages, the main issue remains, that is dealing with the soil-structure interaction of the abutment walls and the supporting piles under various loading condition, especially for

seismic actions.[6] Indeed, the mandate for the revision of the structural Eurocodes, specifically indicated seismic design of IABs among the necessary extension of scope.

In an IAB the concept is to accommodate deck horizontal displacements (e.g., displacements caused by the expansion and contraction due to seasonal temperature fluctuations) with the flexibility of the soil-foundation system rather than with bridge expansion joints. Therefore, in IABs the piles are usually the most flexible elements and are expected to accommodate the lateral movements.[7] This flexibility is provided, usually, using a stub abutment supported by a single row of driven piles or using a frame abutment supported by bored piles. In the long term, due to this cyclic deformations, these bridges experience a buildup of lateral earth pressures on the abutments due to a soil-mechanics phenomenon known as *ratcheting*.[8] Due to this behavior and to limitations of the moment resisting structural scheme, the maximum length of IABs is generally limited.[9–11] Further, from the design point of view, evaluation of the pressure build-up and of the associated internal forces is by no means a trivial task. These difficulties are even more relevant in the seismic case, where for moderate and high seismicity the pressures and forces can be larger than those induced by the thermal movements, dominating the design. For this reason, there is no widely accepted codified analysis method for the seismic design of IABs.

This paper proposes two such practice- and code-oriented equivalent static methods. Section 2 summarizes a non-linear dynamic model (NLDM) in which the soil-structure interaction is approximated by means of non-linear Winkler subgrade, Section 3 presents simplified methods through equivalent static models, while Section 4 illustrates a parameter-sensitivity analysis for the dynamic and the two equivalent static models. Based on this analysis, parameters are selected for the parametric study reported in Section 5, where 5.3 compares the performance of the simplified methods with that of the dynamic one and the prediction error of both models is assessed in terms of bias and coefficient of variation. Finally, 5.4 discusses how partial factors should incorporate these model errors.

Finally, it needs to be remarked how IAB construction practices differ from country to country. In this paper reference is made to the Italian practice, where abutments are of the diaphragm-type, in general quite stiff, and when IABs have multiple spans they are simply supported on sliding bearings over the intermediate piers. Californian practice, or, to remain in Europe, the Slovenian one,[12] have piers that frame into the deck, which is a concrete one. In such cases, piers and abutments share the horizontal seismic action. The basic dynamics of the IAB, as determined from non-linear dynamic analysis, does not change, but for the more simplified method, the equivalent linear one (Section 3.2), iteration might need to be introduced on the earth pressure distribution, for example, similarly to what is done by Vogt[13] in order to achieve consistency between displacements and the sharing of lateral reaction between piers and abutments. This load-sharing is instead an outcome of the analysis in the non-linear static method.

2 | NON-LINEAR DYNAMIC REFERENCE MODEL

In this model the non-linear dynamic behaviour of IABs under seismic action is described by means of non-linear shear springs to account for the site-response in layered soil deposits (called soil-column elements) and non-linear Winkler springs between structural and soil-column elements, to account for soil structure interaction (called interface elements). This model was first proposed by Franchin and Pinto in 2014,[14] later extended in Marchi 2022[15] and calibrated versus high-fidelity FEM in Marchi et al. 2022.[16] Figure 1 shows the model in its main components. The structural elements are modeled as elastic linear, because the focus of the paper is models conceived for design and, according to the second generation Eurocode 8,[17] in this type of bridges structural damage should be prevented due to difficulty in the repair. Non-linear elements can of course be used for structural members and have actually been used in response analysis carried for higher than design intensities (see the risk assessment in Franchin et al.[18]).

The soil-column elements go from the model base at $z = -z_b$ up to the top of the embankment, at $z = H$, in order to model both the deposit site response and the embankment response. There are two soil columns (Figure 1 shows only the right part because the model is symmetric with respect of the center line $x = 0$) and their nodes, with the same depth z, are constrained to have the same horizontal displacements, while vertical displacements of the soil-column nodes are zero. These elements can be considered decoupled from the rest of the model, since the area A_s, and therefore their mass and stiffness are so large that they are not affected by the response of the rest of the system.

Soil-column elements (Figure 1C) have a Bouc-Wen constitutive law, as modified by Gerolymos and Gazetas in 2005[19] to approximate the horizontal non-linear shear behaviour of the soil deposit. This model is defined through the following equations:

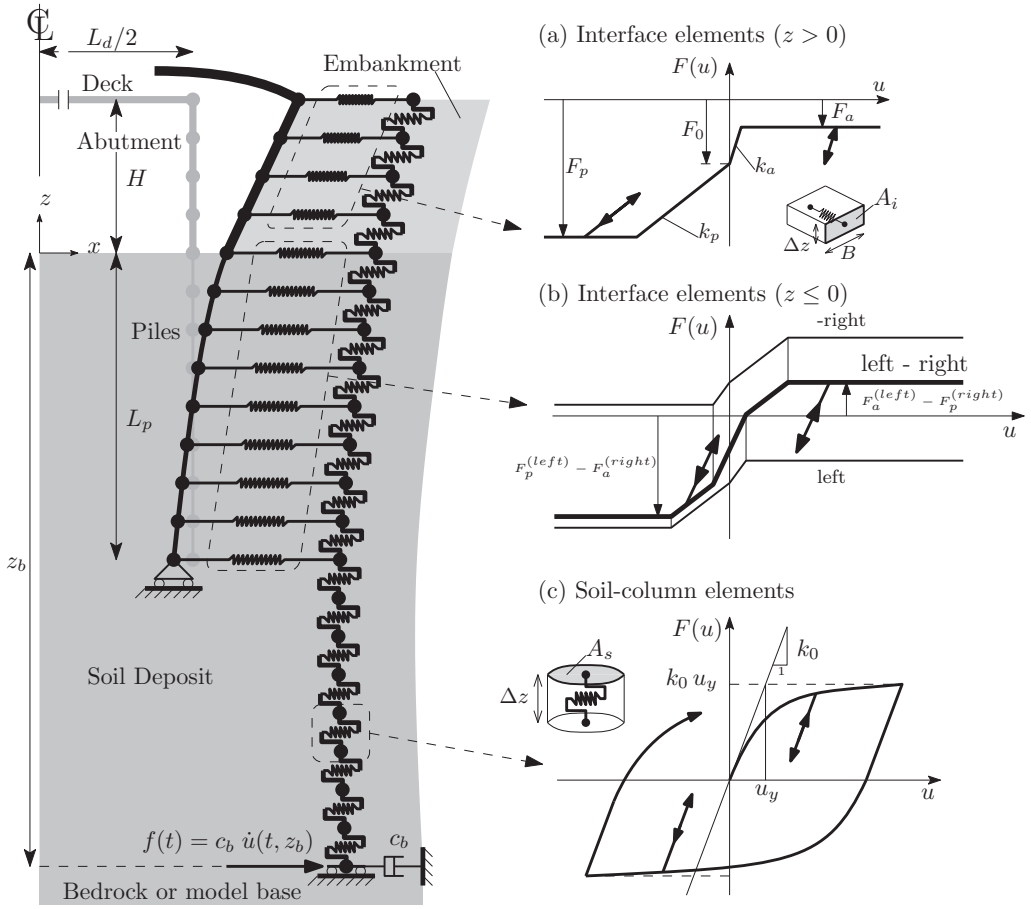

FIGURE 1 NLDM. NLDM, non-linear dynamic model.

$$F(u) = k_0\, u_y\, \zeta(t) \tag{1}$$

$$\frac{\zeta(t)}{\partial t} = \theta\, \frac{u(t)}{u_y} \left\{ 1 - |\zeta(t)|^n \left[\gamma + \beta\, \frac{\dot{u}(t)\, \zeta(t)}{|\dot{u}(t)\, \zeta(t)|} \right] \right\} \tag{2}$$

where the usual Bouc-Wen parameter $A = \gamma + \beta$ is set to unity and the hardening slope ratio α is set to zero.[20] The θ function approximates soil degradation during plasticization and is defined as:

$$\theta = \begin{cases} \dfrac{s_1 + \alpha(\mu_r - 1) + s_2}{s_1 + \mu_r} & \mu_r > s_2 \\ 1 & \mu_r \leq s_2 \end{cases} \tag{3}$$

where s_1 is a dimensionless parameter that controls the stiffness degradation upon stress reversal, s_2 is a characteristic value of "strain ductility" $\mu = \gamma/\gamma_y$ beyond which the effect of θ multiplier on stiffness degradation is activated, and μ_r is a reference strain ductility defined for every unloading or reloading cycle as the ratio of half the difference in strain γ between two previous reversals over the reference strain γ_y. The constitutive parameters of this model (n, γ, β, s_1, s_2 and γ_y) are taken from Drosos et al.[21] as a function of soil type through the plasticity index and confinement pressure σ_0 (spherical part of the stress tensor). Initial stiffness is $k_0 = G_0(z)A_s/\Delta z$, where A_s is the area of soil-column elements (see Figure 1C), G_0 soil low-strain shear modulus, Δz the element height and $u_y = \gamma_y\, \Delta z$ the yielding displacement.

Seismic motion is input to the base of the soil-columns through a velocity proportional force time series applied to linear dampers that model the absorbing boundary at the model base toward incident shear waves,[22] equal to:

$$f(t) = c_b\ \dot{u}(t, -z_b) = [\rho_b\ V_{s,b}\ A_s(-z_b)]\ \frac{\partial u(t, -z_b)}{\partial t} \tag{4}$$

where ρ_b and $V_{s,b}$ are the mass density and shear wave velocity at the model base, respectively, while $A_s(-z_b)$ is the area of the soil-column at its base. The function $\dot{u}(t, -z_b)$ is equal to the outcrop soil horizontal velocity as described in Joyner and Chen.[23]

The horizontal behaviour of the near soil between the abutments and the embankment sufficiently unaffected by the bridge displacement, is approximated by means of non-linear Winkler springs called herein "interface elements". These elements have an elastic perfectly plastic compression-only constitutive law, with non-symmetric strength and stiffness to differentiate for active and passive condition (Figure 1A). The largest compression corresponds to the passive threshold $\sigma'_{h,p} = \sigma'_v\ K_p$. The maximum value (corresponding to the lowest compression) coincides with the active threshold $\sigma'_{h,a} = \sigma'_v\ K_a$. Active and passive conditions differ also in terms of stiffness, defined by the characteristic active and passive lengths l_a and l_p defined in the work of Becci and Nova.[24]

$$l_a = \frac{2}{3}\min(H + L_p; 2H)\tan\left(45^o - \frac{\varphi}{2}\right) \qquad k_a = \frac{1.2\ E_s}{l_a}A_i(z) \tag{5}$$

$$l_p = \frac{2}{3}\min(L_p; H)\tan\left(45^o + \frac{\varphi}{2}\right) \qquad k_p = \frac{1.2\ E_s}{l_p}A_i(z) \tag{6}$$

The values for the active and passive coefficients (K_a and K_p respectively) are taken from the theory of Lancellotta[25] which account also for the friction angle δ between soil and structure (in first approximation this angle can be taken equal to $2/3\ \varphi'$).

In this article IABs with more than one span are also presented. Despite all the configuration possible for the integral abutments and the intermediate piers, the focus is on the Italian practice, where the abutments are reinforced concrete (RC) walls on a row of drilled RC piles and the deck over the intermediate piers is simply supported. Given the particular support configuration the piers are described as a simple support (nodes are constrained only in the z direction).

2.1 | Features of seismic response as assessed by dynamic model

The response of the dynamic model is shown in Figure 2 for the case of a single-span integral abutment highway overpass analyzed in Marchi et al. 2022.[16] The figure shows bending moments time series and displacement profile at the instant of maximum moment at deck-abutments joints for one sample motion and in terms of mode shapes. As it can be seen, because of the very similar static scheme to a moment resisting frame structure, the maximum bending moment on the superstructure is exerted at the deck-abutments joints. While for the piles, the most stressed cross-section is the top one (piles' head). These two quantities, called herein $M_{j,max}$ and $M_{p,max}$ for the maximum bending moment at joints and piles head respectively, are taken as the most relevant in the IAB design and are defined in the following equations:

$$M_{j,max} = \max\left[|M_{\text{left joint}}(t)|, |M_{\text{right joint}}(t)|\right] \tag{7}$$

$$M_{p,max} = \max\left[|M_{\text{left piles}}(t)|, |M_{\text{right piles}}(t)|\right] \tag{8}$$

The first mode of vibration coincides in shape and period with the first vibration mode of the soil deposit. This is consistent with the fact that the column elements have a large enough mass and stiffness to be unaffected by the other elements in the system. It should be noted, however, that this first mode does not impose the largest curvature at the deck-abutments joints and piles' head, a role played by higher modes. This is also shown in terms of frequency spectrum of the system response in Marchi 2022.[15] These higher modes are those where the structural mass leans against the embankment, which reacts limiting the strain and therefore the internal forces in the structure.

Figure 3 illustrates this beneficial aspect of the embankment-abutment interaction by showing the ratio of the maximum bending moments calculated with the embankments to those without the embankments for the two ground motions of Parkfield and Yamakoshi used in Marchi et al.[16] The analysis is carried out varying the deck span length L_d and considering

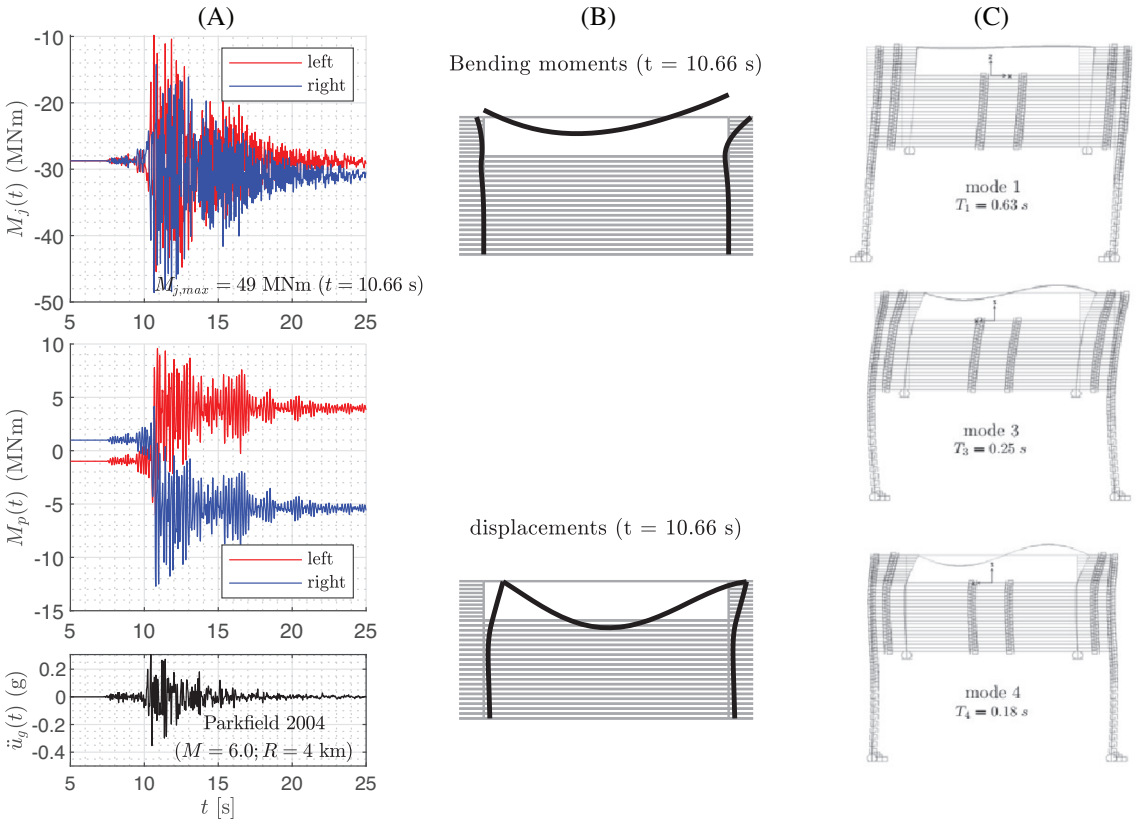

FIGURE 2 Sample dynamic model response: (A) bending moment time series at two locations; (B) bending moment (top) and displacement (bottom) profiles at the time of maximum deck-abutment joint instant; (C) first three mode shapes (mode 2 is related to deck vertical response).

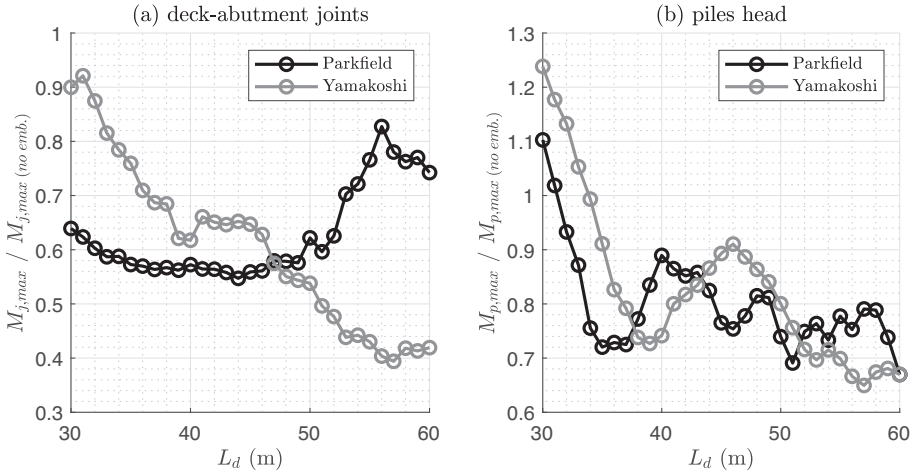

FIGURE 3 Ratio of the maximum bending moment at deck-abutment joints and at piles head (Equations (7) and (8)) obtained with and without the embankments, varying the deck span L_d.

again a single-span case for the sake of illustrating this point. The ratio is always lower than one for $M_{j,max}$ and mostly smaller than one for $M_{p,max}$. The results in Figure 3 are consistent with simple considerations in terms of modal properties: the system without the embankments has longer periods (first mode is related mostly to the deposit) and these correspond to larger spectral displacements and, thus, higher bending moments.

A further important proof of the main role played by higher modes in determining the response of IABs is shown in Figure 4, which illustrates the horizontal absolute acceleration profile averaged over 10 natural motions, selected to be

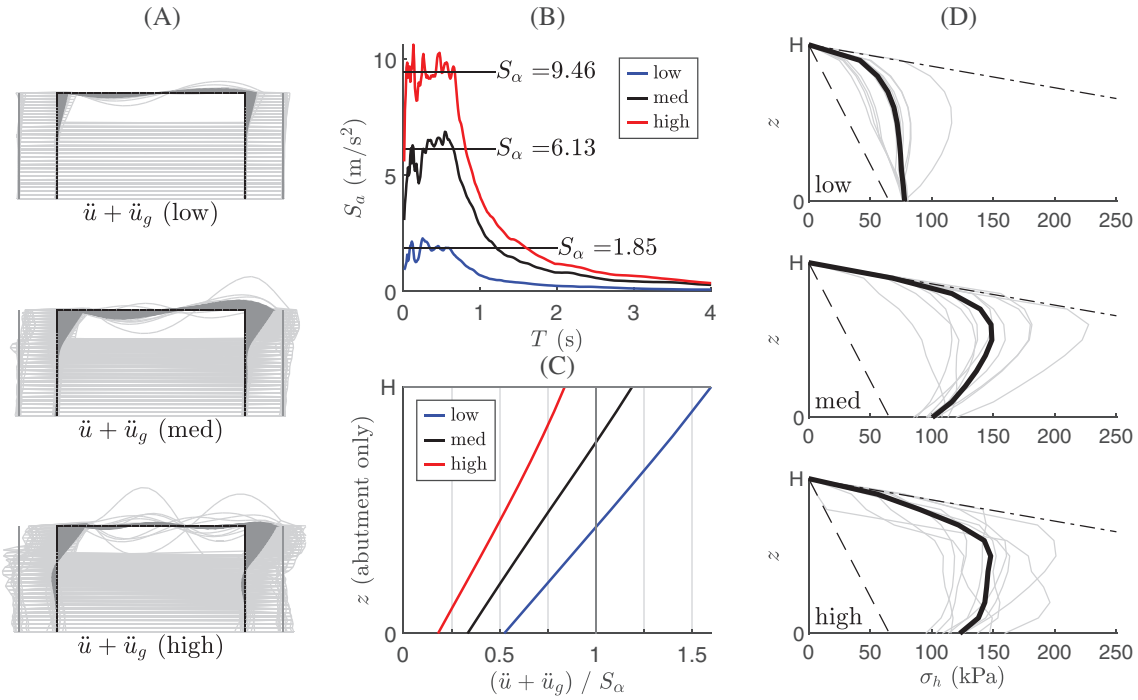

FIGURE 4 Absolute acceleration profiles at time of $M_{j,max}$ for three suites of 10 ground motions each, representative of low, moderate and high seismicity (A); plateau acceleration profiles normalized to the respective S_α (C); earth pressure distributions at time of $M_{j,max}$ for the side against which the bridge leans (D).

spectrum compatible with the design uniform hazard spectrum (T_R = 975 years, highway overpass) at the three Italian sites of Milano, Napoli and L'Aquila used later in the parametric study of Section 5 (the motions are those in Figure 11, the soil profile is always the same). Figure 4A shows a linear profile on the abutments for all cases. Panel (C) shows that this profile, normalized to the plateau acceleration S_α, as assessed in the records ensembles at $z = 0$, that is, including amplitude in panel (B), has maximum value at deck level which is 1.6, 1.2, and 0.8 times S_α for the low, moderate and high seismicity respectively. This constant c can be seen as the product of a participation factor Γ times the modal ordinate ϕ in the assumption that a single mode dominates the response. It is noted for later use how the ratio $\ddot{u}(z = H)/S_\alpha$ decreases with seismic intensity and is on average 1.0 for moderate and high seismicity sites (Naples and L'Aquila). This constant c is also, on average, equal to 0.25 on the abutment bottom section. Figure 4D finally shows the last important output from the dynamic analyses, that is, earth pressure distributions for the 10 ground motions, at each intensity, at the respective time of $M_{j,max}$, and the corresponding average profiles. The shape of these distributions inspires the proposed linear static method in Section 3.2.

2.2 | Scope of application

The models presented in this paper (dynamic model in Section 2 and static models in Section 3) describe only the longitudinal seismic response of straight IABs. Since these bridges are mainly used, due to the structural scheme, for medium and small span bridges like overpasses, the effect of the skew angle must be assessed

To assess the dependency on the skew angle, an extension to 3D of the NLDM presented in Marchi 2022[15] is employed. The deck is modeled through a grillage to account for its spatial behavior in particular, the mass distribution and associated rotational inertia in the deck plane, as well as distributed contact between wall and backfill (the main feature of the dynamic behaviour of skewed bridges is the coupling of the deck in-plane translations and rotations, leading to non-uniform contact pressures). The transversal relative displacements between the embankment and the abutment are modeled through linear elastic spring with stiffness equal to a simple shear model for the embankment wedge although it is common to disregard the tangential component of the response in the modeling of skew bridges, see for example, Kaviani et al.[26] The model is used to perform dynamic analyses for two return periods (T_R = 100 years and T_R = 1000 years) for the site of L'Aquila, with 20 ground motions in each case.

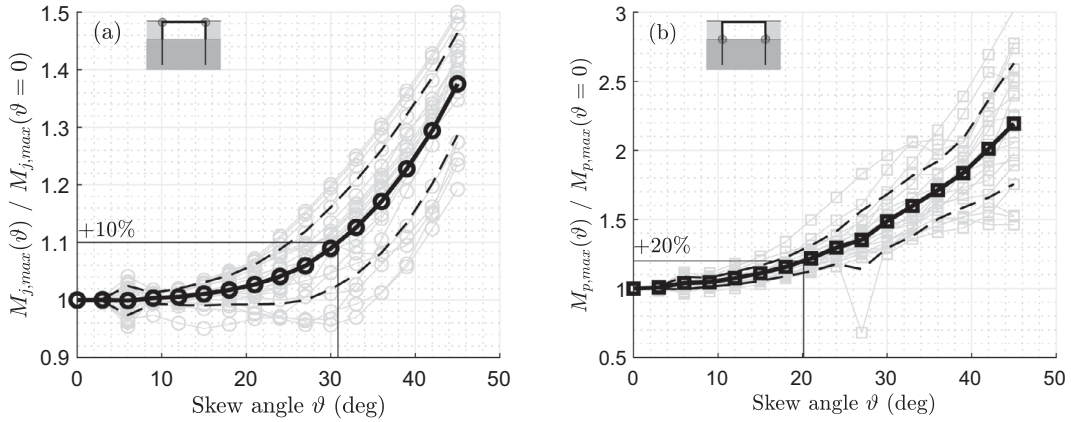

FIGURE 5 Ratio between the maximum bending moment of a skewed and non-skew ($\vartheta = 0$) IAB for $T_R = 100$ years. (A) deck-abutment joints; (B) piles' head. IAB, Integral abutment bridge.

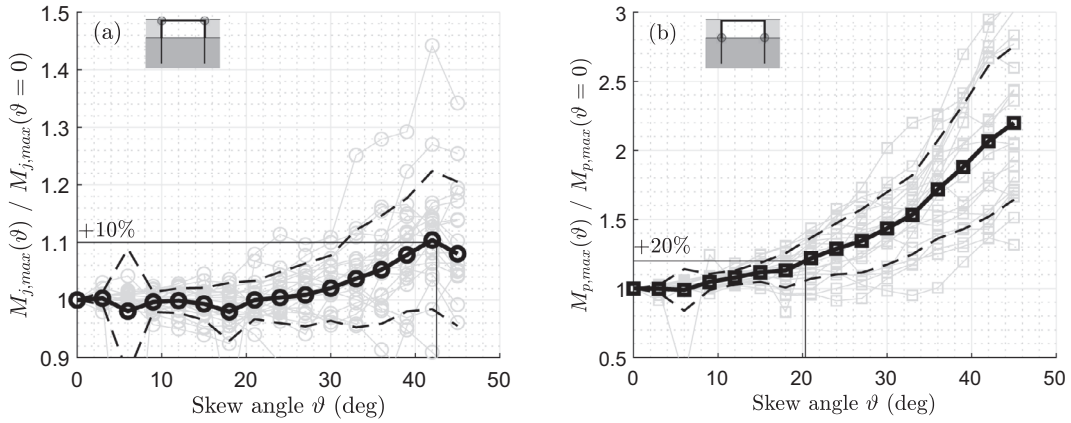

FIGURE 6 Ratio between the maximum bending moment of a skewed and non-skew ($\vartheta = 0$) IAB for $T_R = 1000$ years. (A) deck-abutment joints; (B) piles' head. IAB, Integral abutment bridge.

Figures 5 and 6 show the results in terms of $M_{j,max}$ and $M_{p,max}$, defined in Equations (7) and (8), normalized with respect to the correspondent maximum moments for a skew angle ϑ equal to zero. The results show that the bending moment at the piles head is the response quantity most sensitive to the skew angle ϑ. It increases, on average, about 20% with respect to the case $\vartheta = 0$ for a skew angle of about 20°. This is due in part to the torsional moment on the abutment, caused by the bridge skewness and the horizontal earth pressure, transferred to the piles row. The deck-abutment moment, on the contrary, increases for the same skew angle only about 10% (Figure 5A). For the higher seismic intensity (Figure 6A) the effect of skew on $M_{j,max}$ is even less pronounced. Therefore it can be stated, from the result of these preliminary analyses, that the models presented in this paper for straight IABs can still be applied to integral bridges with skew angles ϑ up to 20° (a threshold for which skewness is often disregarded also in international guidelines, see for example CALTRANS seismic design criteria 2019[27]).

It should be specified that the three-dimensional model, developed as an extension of the two-dimensional one, as opposed to the latter, has not been validated against a higher-order model. However, since the results obtained in terms of the maximum skew angle allowed agree with what is stated by international design codes and applicability restrictions of these bridges, the result of these analyses is evaluated as informative.

3 | EQUIVALENT STATIC MODELS

Static models are based on the idea of representing the system in the configuration where the maximum internal forces are attained. In particular, a non-linear static model (NLSM) that presents the same deformed state as the complete system and

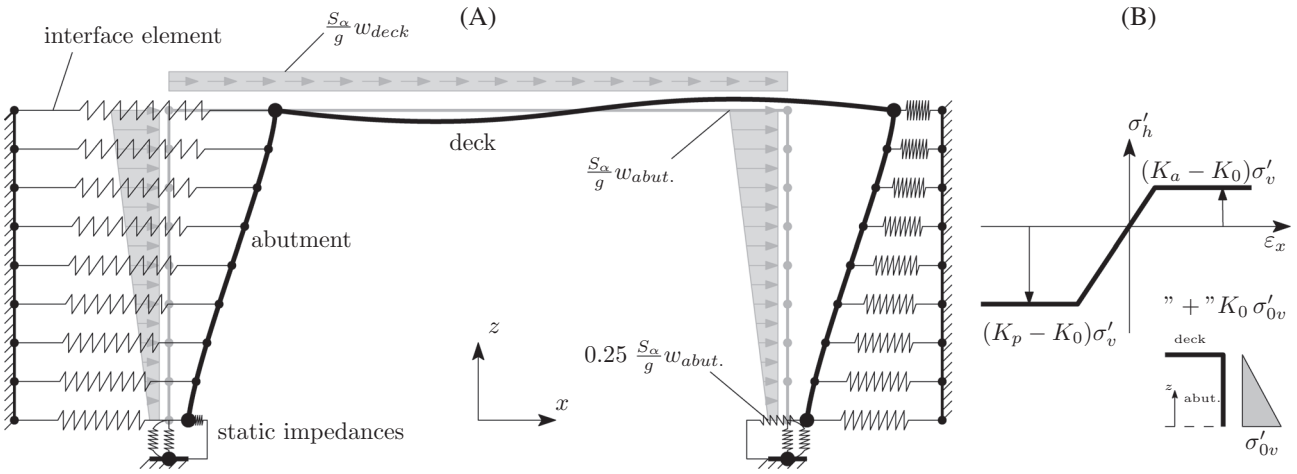

FIGURE 7 NLSM. NLSM, non-linear static model.

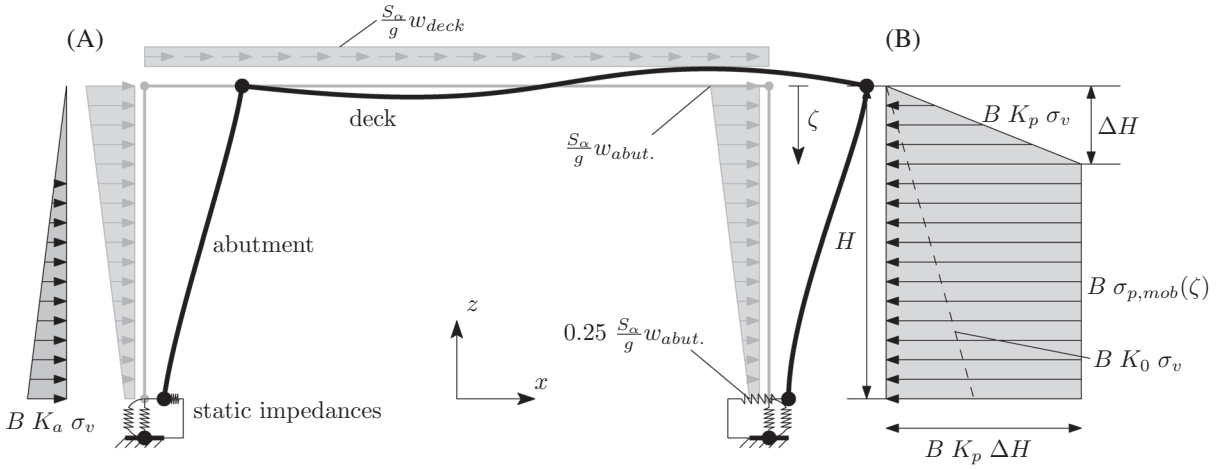

FIGURE 8 LSM: (A) structural inertia forces, (B) bilinear pressure distribution. LSM, linear static model.

a linear static model (LSM) that presents equivalent earth pressure distributions as the NLDM at the instant of maximum bending moments are developed. The concept behind both models is that the bridge, due to the inertia forces, displaces against the embankments that restrain its motion and that occurs in frequencies around those of the first higher modes, as shown in Figures 2 to 4.

To reduce a dynamic model into an equivalent static one it is necessary to introduce explicitly the inertia forces on the structural elements. In the proposed static models this action is assumed as a horizontal distributed load equal to the distributed mass multiplied by the plateau acceleration S_α of the design spectrum for the deck and trapezoidal between $0.25\ S_\alpha/g\ w_{abut.}$ and $S_\alpha/g\ w_{abut.}$ for the abutments (according to Figures 4C, 7 and 8).

Both the static models are derived from a truncation of the complete system at the piles head (non-linear soil elements of NLDM with $z < 0$ are removed). To have the same behaviour in the truncated model as in the complete one, static impedances from literature[28,29] are inserted to account for the removed elements. Static impedances of a single foundation pile (figure A1), are given for a constant and a parabolic stiffness (E_s = const and $E_s = \tilde{E}_s\sqrt{\tilde{z}/d}$ where $\tilde{z}$ is the depth positive downwards) profile as:

$$\text{constant:} \qquad K_{HH} \simeq 1.00\ E_s\ D\left(\frac{E_p}{E_s}\right)^{0.21} \qquad K_{MM} \simeq 0.15\ E_s\ D^3\left(\frac{E_p}{E_s}\right)^{0.75} \qquad K_{HM} \simeq 0.22\ E_s\ D^2\left(\frac{E_p}{E_s}\right)^{0.50} \tag{9}$$

$$\text{parabolic:} \quad K_{HH} \simeq 0.80\,\tilde{E}_s\,D\left(\frac{E_p}{\tilde{E}_s}\right)^{0.28} \qquad K_{MM} \simeq 0.15\,\tilde{E}_s\,D^3\left(\frac{E_p}{\tilde{E}_s}\right)^{0.77} \qquad K_{HM} \simeq 0.24\,\tilde{E}_s\,D^2\left(\frac{E_p}{\tilde{E}_s}\right)^{0.53} \tag{10}$$

where K_{HH} is the pile horizontal stiffness, K_{MM} the flexural stiffness, and $K_{MH} = K_{HM}$ the stiffness of the two coupled degrees of freedom (rocking). E_s is the Young's modulus of the soil, E_p that of the pile, and D the diameter of the pile. The limitations of considering these approximate impedances' expressions lie both in the fact that: (a) in general they only approximately correspond to the actual stiffness variation of the real stratigraphic profile of the deposit, through simplified analytical variations; (b) they do not depend on frequency.

Another important limitation is that group effects are not considered. In fact, static impedances are simply multiplied by the piles number n_p to obtain group impedances. Appendix A presents a simple implementation of static impedances by means of basic finite elements. Finally, it should be emphasized how the use of code-supplied static impedances is likely the largest approximation in both the equivalent static methods, but it is a choice consistent with the anticipated use of the proposed models by practitioners. Clearly the use of more refined formulations for the foundation impedances (not considered herein) would lead to a better match in the piles' bending moments.

Removing the soil-column elements, which incorporate the site-response analysis in the dynamic model, the action (inertia forces on the deck and abutments) is taken either from a code-based response spectrum for the appropriate soil category or from a 1D seismic response analysis for a given set of ground motions.

3.1 | Non-linear static model

In this model the non-linearity is lumped in the interface elements between structure and embankments (Figure 7A). Stress resultants on the structure are calculated through the deformations of the bridge and the interface soil elements reactions.

In commercial finite-element software (such as, e.g., SAP2000) piece-wise linear constitutive laws that do not pass through zero cannot be defined and this might be a problem in the interface element definition. The constitutive law is thus "translated" upwards (see Figure 7B) by extrapolating the contribution of the horizontal stress at rest given by the weight of the embankment on the soil column $F_0(z) = \sigma'_v(z)\,K_0(z)\,A_i(z)$, where $\sigma'_v(z)$ is the vertical effective stress on the soil due only to the embankment weight and $K_0(z)$ the at-rest earth pressure coefficient at depth z.

3.2 | Linear static model

The LSM includes only the structural elements and the foundation static impedances described previously (Figure 8). Soil-structure interaction at the abutment walls is considered through appropriate earth pressure distributions on the abutments.

Due to the relatively small total length of IABs, the longitudinal displacements at the two deck-abutments joints can be assumed equal, therefore while one side attains the active pressure the other (the one towards which the bridge is displacing) has a pressure distribution which is intermediate between the at-rest and the passive state. The pressure distribution is conceived to replicate the qualitative shape of the profiles obtained from the NLDM at different intensities shown in Figure 4D which can be approximated as bilinear, passive up to a certain depth and than constant. Analytically, it can be expressed as:

$$\sigma_{p,mob}(\zeta) = \begin{cases} K_p\,\gamma\,\zeta & \zeta \le \Delta H \\ K_p\,\gamma\,\Delta H & \zeta > \Delta H \end{cases} \tag{11}$$

where the symbols are defined in Figure 8

$$\Delta H = c\,\alpha\,H \qquad \text{with} \qquad \alpha = \frac{S_\alpha(w_{deck}L_{tot} + 2\,w_{abut}H)}{\frac{1}{2}\,g\,\gamma\,H^2\,K_p\,B} \tag{12}$$

where w_{deck} and w_{abut} are the weight per unit length of the deck and the abutments, respectively, L_{tot} is the deck total length, H the abutments height, γ and K_p the embankment unit weight and passive earth pressure coefficient, B abutment

width (in the direction normal to the x–z plane). The constant c depends on the number of spans: for IABs with single span $c = 0.58$, for the two-span case $c = 0.65$; for the three-span case $c = 0.59$. These values are found with a wider parametric study against the NLSM, where all 18 parameters are varied in an extended domain compared to the values listed in Figure 9. Note that Equation (11) refers to a homogeneous embankment in terms of geotechnical parameters.

Note that α has an approximate physical interpretation as the ratio of the structural inertia forces to the resultant of passive pressure distribution developed over the full abutment height. ΔH must obviously increase with increasing α ans c regulates the amount of inertia forces that is resisted by the abutment wall ans the soil behind it and that exerted by the foundations. In particular, the proportion going to the abutment is $\frac{1-(1-c\,\alpha)^2}{\alpha}$. In the following the value 0.6, intermediate for one, two and three-span structures is used, but a value of $c = 0.5$ could be used to avoid under-designing the foundations.

Initially, the model was conceived with a different earth pressure distribution $\sigma_{p,mob}$ which led to an iterative scheme to the evaluation of the model, because it depended on the horizontal displacements of the abutment.[13] Moreover, the previous definition led to a worse performance compared to the bilinear distribution described above despite always in favor of safety (the median of the ratio between the bending moments calculated with the old LSM and the one calculated with the NLDM was always higher than unity).

4 | SENSITIVITY ANALYSIS

A sensitivity analysis has been carried out for the dynamic and the static models to evaluate the parameters with larger influence on the maximum bending moments $M_{j,max}$ and $M_{p,max}$. The candidate parameters considered are: the deck span length L_d and width B, the abutment height H and thickness t_a, , piles diameter D and length L_p, bedrock depth and damper coefficient z_b and c_b, soil unit weight γ, internal friction angle φ' and small-strain shear modulus G_0, horizontal plateau spectral acceleration S_α. The method by Morris used for this analysis indicates qualitatively the most influential parameters and it also gives an indication of the interaction between parameters.[30] It consists of the evaluation of the so called elementary effects associated with i-th parameter and j-th path $EE_i^{(j)}$, which are similar to a numerical approximation of the partial derivatives (tangents) of the target function with respect to the i-th input parameter, normalized to the "secant" $f(\mathbf{x}_i^{(j)})/\mathbf{x}_i^{(j)}$:

$$EE_i^{(j)} = \frac{f\left(\mathbf{x}_i^{(j)}\right) - f\left(\mathbf{x}_{i-1}^{(j)}\right)}{\Delta_i}\left(\frac{x_i^{(j)}}{f\left(\mathbf{x}^{(j)}\right)}\right) \tag{13}$$

where $\mathbf{x}_i^{(j)} = \mathbf{x}_{i-1}^{(j)} + \Delta_i \mathbf{e}_i$ is the value of the parameters' vector at the step in the j-th path taken in the i-th direction, a step of size Δ_i related to the i-th variable and kept constant across all paths, while $\mathbf{x}_{i-1}^{(j)}$ is the value of the parameters' vector at the end of the previous step. Paths are random sequences of n steps, with a single step taken for each of the n variables in the parameters' vector, in random order and starting at any random feasible point. The mean of the elementary effects over these N paths is approximately proportional to the parameter importance, while their standard deviation is related to the interaction between parameters. Morris method is used due to its good performance and because it needs fewer model evaluation compared to others, such as, for example, Sobol[31] and other variance-based methods. The comparatively smaller effort is relevant when models (like the dynamic model in Section 2, are costly to evaluate). Table 1 shows the results in terms of the mean absolute value of the elementary effects $\mu_i^* = \frac{1}{N}\sum_{j=1}^{N} |EE_i^{(j)}|$ and their standard deviation $\sigma_i = \sqrt{\frac{1}{N-1}\sum_{j=1}^{N}(EE_i^{(j)} - \mu_i)^2}$ where $\mu_i = \frac{1}{N}\sum_{j=1}^{N} EE_i^{(j)}$ is the arithmetic mean of the elementary effects of the i-th parameter over all the N samples.[32]

Bold values indicate the first four most important parameters (higher μ^*): the first in the dynamic and static models, is deck length L_d. The abutment thickness t_a is also the second most relevant parameter while static models are affected also by the plateau spectral acceleration S_α. This sensitivity of both dynamic and static models is partially caused by the sensibility of the model response to the ratio between the deck and the piles-abutments flexural stiffness (in fact also the piles diameter D, which concur in the evaluation of the piles horizontal stiffness, has a high value of μ^*). The dynamic model seems to be insensible to the soil and bedrock parameters z_b, γ, φ', c_b, and G_0 and this is consistent with the observation that the model response is not governed by the first mode (first soil-deposit mode)

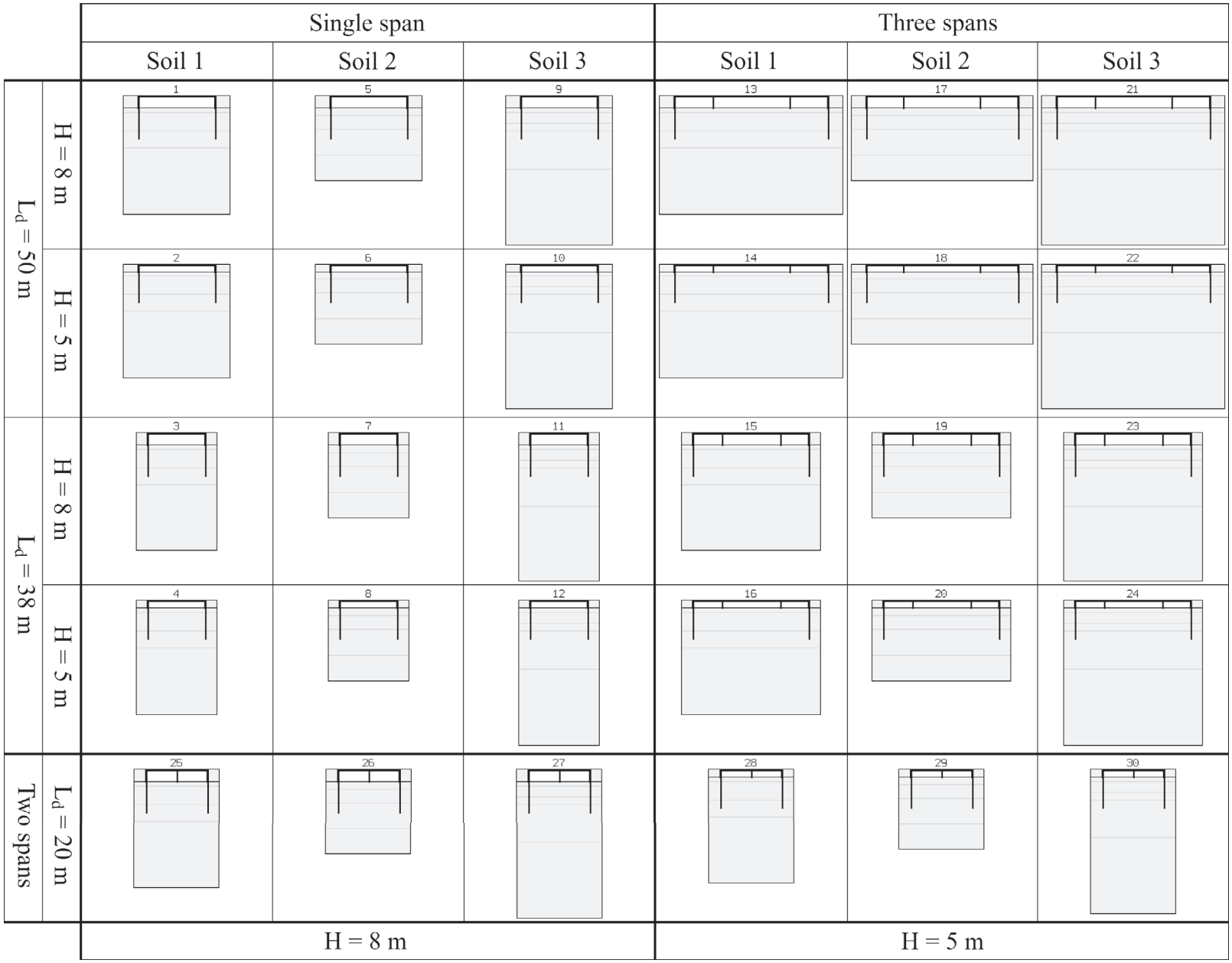

FIGURE 9 Cases considered in the parametric comparative study.

TABLE 1 Sensitivity analysis results using Morris method.[33] Models output is calculated in terms of maximum bending moments at deck-abutment joints $M_{j,max}$ and at piles head $M_{p,max}$.

	$M_{j,max}$						$M_{p,max}$					
	NLDM		NLSM		LSM		NLDM		NLSM		LSM	
param.	μ^*	σ	μ^*	σ	μ^*	σ	μ^*	σ	μ^*	σ	μ^*	σ
L_d	**1.84**	0.61	**1.77**	0.11	**1.76**	0.12	0.92	0.09	0.82	0.98	1.39	1.59
B	0.08	0.05	0.04	0.05	0.10	0.13	0.29	0.06	0.33	0.40	0.46	0.48
H	**0.10**	0.04	0.05	0.05	**0.21**	0.10	1.52	0.82	1.13	1.22	1.76	1.75
t_a	**0.14**	0.20	**0.23**	0.07	0.14	0.15	0.64	0.43	0.47	0.42	0.51	0.48
L_p	0.01	0.01	0.00	0.00	0.00	0.00	0.00	0.00	0.00	0.00	0.00	0.00
D	**0.11**	0.50	**0.11**	0.07	0.16	0.05	1.82	1.32	1.82	0.37	1.34	0.33
z_b	0.09	0.04	–	–	–	–	0.18	0.01	–	–	–	–
c_b	0.08	0.37	–	–	–	–	0.21	0.16	–	–	–	–
γ	0.05	0.09	–	–	–	–	0.00	0.03	–	–	–	–
φ'	0.04	0.00	–	–	–	–	0.11	0.01	–	–	–	–
G_0	0.00	0.00	0.00	0.00	0.00	0.00	0.00	0.00	0.11	0.08	0.00	0.00
S_α	–	–	**0.32**	0.12	**0.31**	0.14	–	–	0.99	0.41	1.22	0.75

Abbreviations: LSM, linear static model; NLDM, non-linear dynamic model; NLSM, non-linear static model.

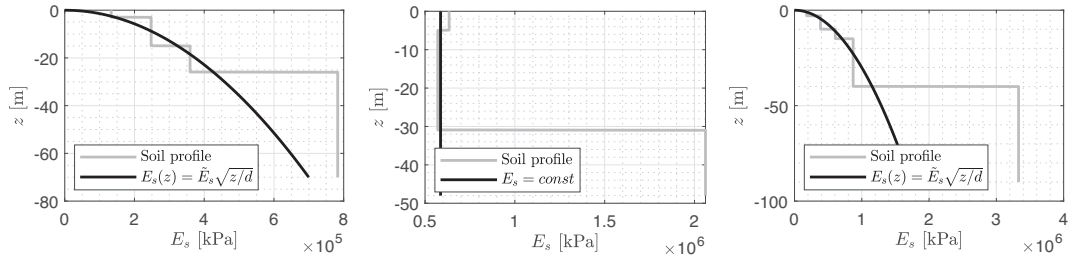

(A) Soil 1: Milano ($\tilde{E}_s = 92$ MPa)

(B) Soil 2: Napoli ($E_s = 586$ MPa)

(C) Soil 3: L'Aquila ($\tilde{E}_s = 200$ MPa)

FIGURE 10 Soil profiles in terms of elastic modulus E_s and the fitted profile for the evaluation of the static impedances[28] for the three Italian sites of Milano, Napoli, and L'Aquila.

which depends on the deposit thickness z_b, its unit weight γ and shear modulus G_0. From Table 1 emerges that the most important parameters to include in the parametric study are: structural dimensions L_d, H and t_a; soil properties (despite the low sensitivity cannot be ignored); pile diameter D. Abutment thickness t_a can be defined as function of L_d, H and number of spans, while D can be considered equal to 1.2 m for the piles used in typical bridges foundations in Italy.

5 | PARAMETRIC STUDY

To validate of the proposed static models, a parametric analysis was performed to cover a representative range of integral abutment overpasses in terms of number of spans, main span length L_d (when there are three spans the side ones have length equal to $L_d/2$), abutment height H and soil profile. All the cases are listed in Figure 9 and the parameters values were chosen to be representative of typical integral abutment solutions proposed for Italian highway overpasses.[34] Soil profiles used are characteristic for the sites of Milano, Napoli, and L'Aquila, taken as representative of low, moderate, and high seismicity, respectively, for the Italian territory.[18] For the definition of the static impedances used in the static model,[28] the parabolic profiles for soils 1 and 3 and the constant profile for soil 2 were taken; as shown in Figure 10. Note that the impedance profiles (in black) are fitted only in the shallow part of the profile; for a depth equal to the piles length L_p.

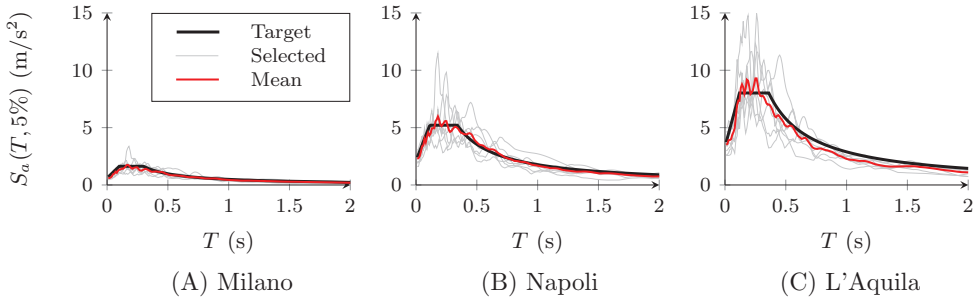

FIGURE 11 Target spectrum (black) and selected ground motions spectra (grey) with their average (red).

TABLE 2 Plateau acceleration for the three sites and three intensities considered before (italics) and after the site-response analysis for the three soil profiles.

	MI	NA	AQ
$S_{\alpha,bedrock}$	*0.17*	*0.53*	*0.82*
Soil 1 (MI)	0.31	0.99	1.49
Soil 2 (NA)	0.21	0.71	1.17
Soil 3 (AQ)	0.29	0.99	1.56

Note: Values are expressed in g.

5.1 | Seismic input

Seismic ground motions were selected to match the Italian code spectra for three seismic intensity levels (low, medium and high characterized by a PGA of 0.1, 0.2 and 0.35 g respectively) on rock/stiff soil at each of the three sites. For the purpose of static analyses, that is, in order to determine S_α at the bridge level ($z = 0$), these ground motions have been used as input to one-dimensional site response analysis with the chosen profiles without the embankments. The acceleration spectra of the selected GMs, together with their average spectrum, are compared to the code target spectrum in Figure 11. The code spectra refer to a return period T_R of 975 years, appropriate for highway overpasses, on rock (soil A according to Eurocodes classification). The return period of 975 years is chosen in accordance with the Italian code for the life-safe limit state of highway structures (higher than ordinary importance), that is, with an exceeding probability of 10% in 100 years (in place of the usual 50 years).

Table 2 lists the values of the plateau acceleration S_α for the three sites and the three intensities. The first row reports $S_{\alpha,bedrock}$, which is the value on rock/stiff soil, that is, the value from the target spectra used in GM selection (Figure 11). The remaining three rows report the average of the spectral acceleration values obtained after site-response analysis for each of the selected ground motion. The average is performed over the range of periods $[T_B, T_C]$ of the target code spectrum, and it is thus the best estimate of S_α at the surface, that is, the value to be used for static analysis.

5.2 | Modal properties from the dynamic model

Figure 12 shows the vibration periods of the first 10 modes calculated using the NLDM. As it can be seen, apart from the period of the first mode, which correspond to the fundamental soil deposit mode, higher ones fall within the $[T_B, T_C]$ range of periods at which plateau acceleration occurs for the target spectra used in input ground motions selection (i.e., $T_i \in [0.1\text{ s}, 0.35\text{ s}]$ for $i = 2, 3, 4, 5$). Since the structural response of this type of bridges is more influenced by the higher modes, as pointed out previously, this corroborates the proposal of using S_α in the static methods.

5.3 | Comparison of internal forces

Figure 13 and Figure 14 shows the relationships between the maximum bending moment at deck-abutment joints (abutment top cross-section) $M_{j,max}$ and the maximum bending moment at piles head (abutment bottom cross-section) $M_{p,max}$

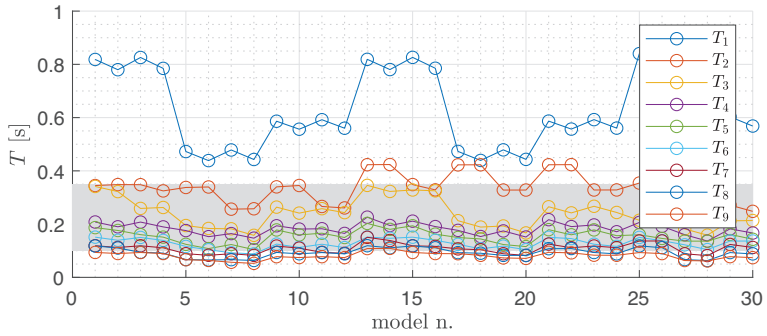

FIGURE 12 Modal properties of the NLDM. Plateau range of periods between $[T_B, T_C]$ of the target spectra of Figure 11 are indicated with shaded area. NLDM, non-linear dynamic model.

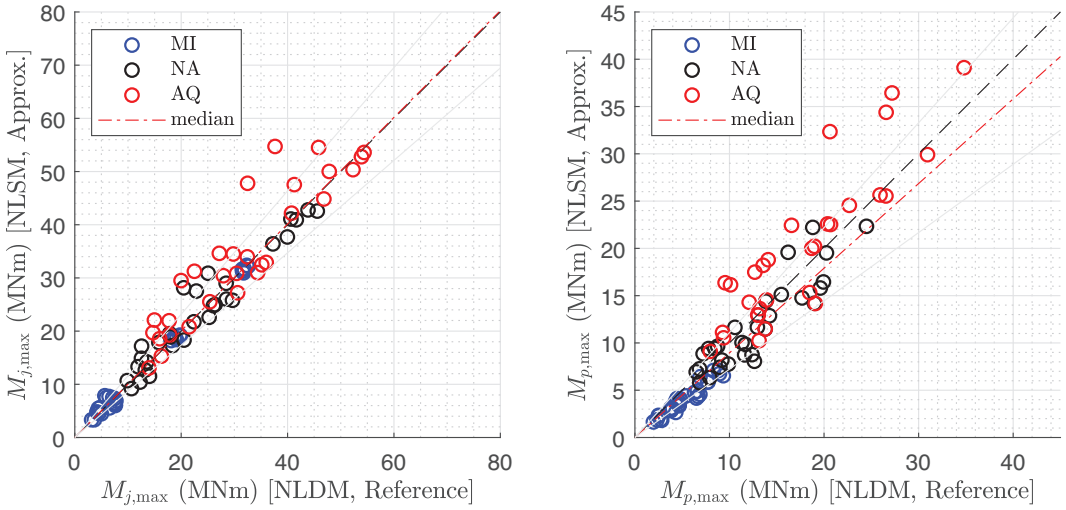

FIGURE 13 Comparison between NLDM and NLSM in terms of bending moment at abutment top cross-section $M_{j,max}$ and at piles head $M_{p,max}$. NLDM, non-linear dynamic model; NLSM, non-linear static model.

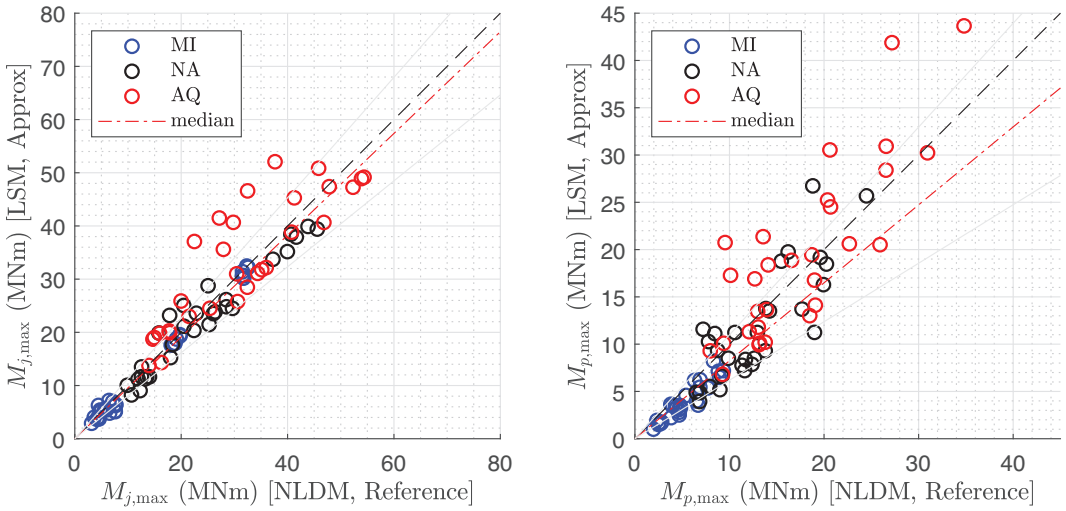

FIGURE 14 Comparison between NLDM and LSM in terms of bending moment at abutment top cross-section $M_{j,max}$ and at piles head $M_{p,max}$. LSM, linear static model; NLDM, non-linear dynamic model.

TABLE 3 Statistic comparison of the ratio between static and dynamic models response in terms of maximum bending moment.

Model	Section	Median	CV	Correlation
NLSM	Joint	1.00	0.16	0.96
NLSM	Piles	0.90	0.24	0.94
LSM	Joint	0.96	0.18	0.95
LSM	Piles	0.82	0.33	0.91

Abbreviations: LSM, linear static model; NLSM, non-linear static model.

obtained using the dynamic model (NLDM) and static models (NLSM and LSM) over all cases listed in Figure 9. The figures shows on the abscissae the dynamic model results and, on the ordinates, those computed via static models. The 1:1 line indicates a perfect agreement between the models in terms of response parameter $M_{j,max}$ and $M_{p,max}$. Red, black and blue markers are associated with the seismic intensity level. For the two and three span cases, since the intermediate piers are simply supported, the nodes over the piers are constrained only in the z direction displacement.

As it can be seen from Figures 13 and 14 there is a good match between dynamic and static models for both the maximum bending moments on the deck-abutment joints and at the piles head. Table 3 shows the statistical parameters of the ratio $M_{\text{static model}}/M_{\text{dynamic model}}$. CV is the coefficient of variation and the correlation is calculated between dynamic and static model results by the Pearson correlation coefficient $\rho_{XY} = COV(X,Y)/(\sigma_X\ \sigma_Y)$ where $COV(X,Y)$ is the covariance between X and Y and σ_X, σ_Y are the two standard deviations.

Linear static method is characterized by a coarser approximation compared to the other two models due to the static impedance definition and approximated earth pressure. In fact the influence of the base impedance approximation in LSM is higher due to the absence of the soil interfaces.

5.4 | Partial safety factor to account for modeling uncertainty

The parametric study covers different intensities, number and length of spans, abutment heights and, finally, soil profiles. The characterization of the median and coefficient of variation of the ratio of simplified-to-reference model response over all these cases supports calibration of a lognormal model error term Θ. The latter can be employed to establish values for a partial safety factor to be used in design.[35]

In general terms, a load-side and a resistance-side partial factors should be used in limit-state design, including the seismic one. The former factor, γ_{Ed}, applied to the representative value of the action-effect yields its design value, E_d, and the latter, γ_{Rd}, applied to the representative value of resistance provides its design value, R_d. As pointed out in Franchin and Noto,[36] however, design to EN1998[17] does not include a load-side factor on the seismic action effect, unlike those used on permanent (dead) and variable (live, wind or snow) load effects, γ_G and γ_Q, for the corresponding design. For this reason, a single resistance-side partial safety factor was proposed therein to account for the total uncertainty. In principle, all simplified design methods, including, for example, modal response spectrum analysis or equivalent linear static analysis, should be characterized with a model error, in a way similar to what was done in the previous section for the proposed analysis methods, that is, comparing predicted action effects with those obtained from a reference higher-level method (non-linear dynamic for the seismic case, possibly on a reliable model, like the one calibrated versus even higher order FEM in this case). Since this is not done consistently over all methods, it cannot be proposed only for the methods presented herein, since it would unjustifiably introduce a penalization in the design process of otherwise robust and well-performing structures such as IABs. But just to make the point, with the information in the previous section, and data from Franchin and Noto,[36] a load-side factor for the seismic action effects, for example, the deck-abutment joint and piles' head moments M_j and M_p, can be derived in the form:

$$\gamma_{Ed} = \exp\left(\alpha_E^2\,\beta_{tgt}\,\sigma_T\right)\ \exp\left(-\kappa_E\,\sigma_E\right) \tag{14}$$

where α_E is the action-effect sensitivity factor, β_{tgt} is the target reliability index in the reference period and for the considered limit state,[37] κ_E is the number of logarithmic standard deviations from the log-mean of the action-effect fractile E_k, function of the corresponding number of log-standard deviations for the seismic action intensity for the considered LS, S_k, denoted as κ_S. Terms σ_T and σ_E are the total and the action effect logarithmic standard deviations, respectively, given

by:

$$\sigma_T = \sqrt{\sigma_E^2 + \sigma_R^2} \tag{15}$$

with σ_R the log-standard deviation of the resistance, and:

$$\sigma_E = \sqrt{\sigma_S^2 + \sigma_{E|S}^2} \tag{16}$$

In the last equation, σ_S and $\sigma_{E|S}$ represent the uncertainty in the seismic action intensity measure, for example, the spectral acceleration at the fundamental period, $S_a(T_1)$, and the so-called record-to-record variability, that is, the uncertainty in the effect E conditional on $S_a(T_1)$. The uncertainty σ_S is related to the hazard slope and therefore to the considered spectral ordinate and seismicity of the site, varying between about 0.5 and 1.0.[36] The record-to-record variability can be safely assumed to be constant and about 0.3 (Cornell et al., 2002[38]). Overall, σ_E varies between about 0.6 and 1.1. The corresponding uncertainty on resistance depends on the considered failure mode and severity of damage (i.e., LS) and varies between about 0.2 and 0.5.

Using the average value $\overline{\alpha}_E = -0.91$, appropriate for the seismic design situation[36]; a value of $\beta_{tgt} = 1.76$ for the reliability index in 50 years, appropriate for the design of highway bridge structures (consequence class, or CC, 3a in the Eurocode) at the significant damage or life safety LS,[17,37] and the corresponding return period of the seismic action of $T_R = 600$ years[1], that is, $\kappa_S = 1.4$ and therefore $\kappa_E = 1.3$; values of $\sigma_E = 0.85$ and $\sigma_R = 0.35$, finally yields $\gamma_{Ed} = 1.26$.

The additional contribution of the lognormal model error Θ due to the equivalent static method of analysis modifies the previous expressions in:

$$\sigma_E = \sqrt{\sigma_S^2 + \sigma_{E|S}^2 + \sigma_\Theta^2} \tag{17}$$

$$\gamma_{Ed} = \frac{\exp\left(\alpha_E^2 \beta_{tgt} \sigma_T\right) \exp\left(-\kappa_E \sigma_E\right)}{\mu_\Theta} \tag{18}$$

Using the values for the NLSM from Table 3, $\mu_\Theta = 1.0$ and $\sigma_\Theta = 0.16$ (for the latter the log-standard deviation is taken equal to the coefficient of variation) for the deck-abutment joint and $\mu_\Theta = 0.9$ and $\sigma_\Theta = 0.24$ for the piles' head, provides $\sigma_E = 0.87$ and $\sigma_E = 0.88$ leading to negligible differences in γ_{Ed}. The only case where considering the model error would be needed is that of the linear static model, at the piles' head, where $\mu_\Theta = 0.82$ and $\sigma_\Theta = 0.33$, leading to $\sigma_E = 0.92$ and $\gamma_{Ed} = 1.42 > 1.26$, which amounts to a 13% increase in action effect. In can be concluded that using the proposed equivalent NLSM does not require any specific precaution with respect to safety margins, and that the linear static one can be used by increasing the piles' head moment from analysis.

6 | CONCLUSIONS

This paper presented two simplified design-oriented methods to analyze the longitudinal seismic response of IABs: both are equivalent static methods, one non-linear and the other linear. The starting point for these proposals is the observation of IAB's response from a NLDM, previously developed by the authors. The main aspect of the dynamic response, as highlighted by this model (which has been at least compared with high-fidelity non-linear dynamic FEM), are that the larger structural deformation and, thus, internal forces, develop due to higher modes which are structure-embankment modes. Analysis of the acceleration profiles and earth pressure distributions led to the proposal of equivalent lateral forces, for both methods, and of the pressure distribution for the linear one.

Analysis of the three-dimensional version of the NLDM for increasing skew angles allowed to define the scope of application of the proposed methods, which can be used up to the commonly adopted limit of 20°.

Sensitivity analysis has also been carried out to determine for all three models the most relevant parameters and set up a parametric study to compare the response, in terms of design internal forces, from the simplified static methods and the reference dynamic one. This resulted in a total of 30 cases, including single-, two- and three-span cases; low, moderate

[1] Note that in this discussion the return period for highway overpasses, still considered more important than ordinary structures (CC3a rather than CC2) is set to 600 years according the second generation Eurocode 8 Part 1-1, whereas comparison of results of equivalent static and dynamic analyses was carried out for 975 years (Italian code). This has no influence on the conclusions.

and high seismicity; three different non-homogeneous soil profiles and varying abutment height and span lengths. The results of this study led to model error characterization in terms of bias (small) and coefficient of variation (smaller for the non-linear method, as expected). This additional model uncertainty is then considered in terms of its incremental effect with respect to other components of the total uncertainty, such as the uncertainty in the intensity measure and the record-to-record variability, leading to the conclusion that the proposed methods can be employed in practice without the need for specific modifications to the safety format. Future research on design-oriented methods could focus on simplified procedures to account for thermal moments and their combination with seismic ones.

Finally, it is once again remarked that even though the IAB configurations considered are representative of Italian practice, whereby abutments are of the strong diaphragm type, decks are mostly composite steel-concrete ones, and supported on sliding bearings over the intermediate piers, the non-linear static method is applicable as is also in the case of piers framing into a concrete deck, or in any case restraining it against lateral movements, thus taking part in the lateral-load resisting mechanism.

ACKNOWLEDGMENTS

The study received financial support from the Dipartimento della Protezione Civile, Presidenza del Consiglio dei Ministri, via the Reluis network, granted through the Research projects 2019–2021 and 2022–2023. The authors are grateful for valuable discussions with Prof. Luigi Callisto, Dr Davide Noé Gorini and Dr Fabrizio Noto.

DATA AVAILABILITY STATEMENT

The data that support the findings of this study are available from the corresponding author upon reasonable request.

ORCID

Andrea Marchi https://orcid.org/0000-0001-6645-3633
Paolo Franchin https://orcid.org/0000-0002-1995-0415

REFERENCES

1. Dicleli M, Erhan S. Low cycle fatigue effects in integral bridge steel H-piles under seismic displacement reversals. *Bridge Struct*. 2013;9:185-190. doi:10.1007/978-81-322-2187-6_192
2. Caristo A, Barnes J, Mitoulis S. Numerical modelling of integral abutment bridges under seasonal thermal cycles. *Proc Inst Civil Eng – Bridge Eng*. 2018;171(3):179-190. doi:10.1680/jbren.17.00025
3. Waldin J, Jennings J, Routledge P. Critically, damaged bridges with integral abutments. In: Proceedings of the New Zealand Society for Earthquake Engineering Annual Conference, New Zealand, 1987:1-8.
4. Wood J. Earthquake design of bridges with integral abutments. In: Proceedings of the 6th International Conference on Earthquake Engineering. Christchurch, New Zealand, 2015.
5. Nishida H, Hirozaku M, Shinya K, Tetsuya K, Toshiaki N, Shoichi N. Design and construction guideline of integral abutment bridges for Japanese highways. In: Proceedings of the 28th US-Japan Bridge Engineering Workshop. Tsukuba, Japan, 2012.
6. Dhar S, Dasgupta K. Seismic soil structure interaction for integral abutment bridges: a review. *Transp Inf Geotech*. 2019;6(4):249-267. doi:10.1007/s40515-019-00081-y
7. Erhan S, Dicleli M. Effect of dynamic soil–bridge interaction modeling assumptions on the calculated seismic response of integral bridges. *Soil Dyn Earthq Eng*. 2014;66:42-55. doi:10.1016/j.soildyn.2014.06.033
8. Lafave J, Riddle J, Jarrett M, et al. Numerical simulations of steel integral abutment bridges under thermal loading. *J Bridge Eng*. 2016;21(10). doi:10.1061/(ASCE)BE.1943-5592.0000919
9. Dicleli M, Eng P, Albhaisi S. Maximum length of integral bridges supported on steel H-piles driven in sand. *Eng Struct*. 2003;25(12):1491-1504. doi:10.1016/S0141-0296(03)00116-0
10. Zordan T, Briseghella B, Lan C. Analytical formulation for limit length of integral abutment bridges. *Struct Eng Int*. 2011;21(3):304-310. doi:10.2749/101686611X13049248220654
11. Baptiste K, Kim W, Laman J. Parametric study and length limitations for prestressed concrete girder integral abutment bridges. *Struct Eng Int*. 2011;21(2):151-156. doi:10.2749/101686611X12994961034219
12. Isankovic T. Personal communication. 2023.
13. Feldmann M, Naumes J, Pak D, et al. Design Guide Integral Bridges, Economic and Durable Design of Composite Bridges with Integral Abutments. CEN/TC 250/SC 10; 2010. EN 1990 Basis of structural design.
14. Franchin P, Pinto P. Performance-based seismic design of integral abutment bridges. *Bull Earthquake Eng*. 2014;12:939-960. doi:10.1007/s10518-013-9552-2
15. Marchi A. *Simplified Seismic Analysis of Straight Integral Frame-Abutment Bridges*. PhD dissertation. Sapienza University of Rome; 2022.
16. Marchi A, Gallese D, Gorini D, Franchin P, Callisto L. On the seismic performance of integral abutment bridges: from advanced numerical modelling to practice-oriented analysis method. *Earthquake Eng Struct Dyn*. 2022;52(1):164-182. doi:10.1002/eqe.3755

17. CEN. *Eurocode 8 – Design of Structures for Earthquake Resistance. Part 1-1: General Rules and Seismic Action*. European Committee for Standardization, Technical Committe 250, Sub-Committe 8; 2023. Technical report N1254.
18. Franchin P, Baltzopoulos G, Biondini F, et al. Seismic reliability of Italian code-conforming bridges. *Earthquake Eng Struct Dyn*. 2023;52(14):4442-4465. doi:10.1002/eqe.3958
19. Gerolymos N, Gazetas G. Constitutive model for 1-D cyclic soil behaviour applied to seismic analysis of layered deposits. *Soils Found*. 2005;45(3):147-159. doi:10.3208/sandf.45.3_147
20. Marchi A. Improved Bouc-Wen model implementation in OpenSees. In: *Lecture Notes in Civil Engineering*. Vol 326. Springer; Proceedings of the 2022 Eurasian OpenSees Days. Torino, Italy; 2022:31-38. doi:10.1007/978-3-031-30125-4_3
21. Drosos V, Gerolymos N, Gazetas G. Constitutive model for soil amplification of ground shaking: parameter calibration, comparison, validation. *Soil Dyn Earthquake Eng*. 2012;42:255-274. doi:10.1016/j.soildyn.2012.06.003
22. Lysmer L, Kuhlemeyer R. Finite dynamic model for infinite media. *ASCE Knl Eng Mech Div*. 1969;4:859-977. doi:10.1061/JMCEA3.0001144
23. Joyner W, Chen A. Calculation of nonlinear ground response in earthquakes. *Bull Seismol Soc Am*. 1975;65(5):1315-1336. doi:10.1785/BSSA0650051315
24. Becci B, Nova R. A method for analysis and design of flexible sheetpiles. *Riv Ital Ginecol*. 1987;87:33-47.
25. Lancellotta R. Analytical solution of passive earth pressure. *Géotechnique*. 2002;52(8):617-619. doi:10.1680/geot.2002.52.8.617
26. Kaviani P, Zareian F, Taciroglu E. Seismic behavior of reinforced concrete bridges with skew-angled seat-type abutments. *Eng Struct*. 2012;45:137-150. doi:10.1016/j.engstruct.2012.06.013
27. CALTRANS. Seismic design criteria (version 2). US; 2019.
28. Gazetas G. Foundation vibration. In: *Foundation Engineering Handbook*. pp. 553-593. Springer; 1991.
29. CEN. *Eurocode 8 – Design of Structures for Earthquake Resistance. Part 5: Geotechnical Aspects, Foundations, Retaining and Underground Structures*. European Committee for Standardization, Technical Committe 250, Sub-Committe 8; 2022. Technical report N1092.
30. Morris M. Factorial sampling plans for preliminary computational experiments. *Technometrics*. 1991;33(2):161-174. doi:10.1080/00401706.1991.10484804
31. Sobol I. Global sensitivity indices for nonlinear mathematical models and their Monte Carlo estimates. *Math Comput Simulat*. 2001;55(1-3):271-280. doi:10.1016/S0378-4754(00)00270-6
32. Campolongo F, Cariboni J, Saltelli A. Sensitivity analysis: the Morris method versus the variance based measures. *Technometrics*. 2003.
33. Saltelli A, Tarantola S, Campolongo F, Ratto M. *Sensitivity Analysis in Practice a Guide to Assessing Scientific Models*. Joint Research Centre of the European Commission, Ispra, Italy, John Wiley & Sons, Ltd; 2004.
34. Torricelli LF, Marchiondelli A, Pefano R, Stucchi R. Integral bridge design solutions for Italian highway overpasses. In: Proceedings of the Sixth International IABMAS Conference, Stresa, Italy, 2012.
35. CEN. *EN 1990 – Eurocode - Basis of Structural and Geotechnical Design*. European Committee for Standardization, Technical Committe 250; 2020. Technical report N2555.
36. Franchin P, Noto F. Reliability-based partial factors for seismic design and assessment consistent with second-generation Eurocode 8. *Earthq Eng Struct Dyn*. 2023. doi:10.1002/eqe.3840
37. Franchin P, Noto F. Partial factors for displacement-based seismic design and assessment consistent with the second-generation of Eurocodes. In: 14th International Conference on Applications of Statistics and Probability in Civil Engineering (ICASP14), Dublin, Ireland, 2023.
38. Cornell A, Jalayer F, Hamburger R, Foutch D. Probabilistic basis for 2000 SAC Federal Emergency Management Agency Steel Moment Frame Guidelines. *J Struct Eng*. 2002;128(4):526-533. doi:10.1061/(ASCE)0733-9445(2002)128:4(526)

How to cite this article: Marchi A, Franchin P. Equivalent static methods for seismic design of straight integral abutment bridges. *Earthquake Engng Struct Dyn*. 2023;1-19. https://doi.org/10.1002/eqe.4052

APPENDIX: STATIC IMPEDANCES MODELING IN FINITE ELEMENT SOFTWARE

The static impedances used to discretize the behaviour of piles and the surrounding soil interacting with them in static analysis methods described in Section 3 can be modeled in various ways into finite element software. Impedances are linear elastic elements in which the stiffness is defined through a matrix since there are coupling components between the translational and rotational degree of freedoms. Since for the piles the behaviour is mainly coupled in the horizontal component, the static impedances are defined through the system of equations outlined in Figure A1.

Decoupled from the horizontal-rotational behaviour $(u - \phi)$ is also present the vertical one, defined through the stiffness K_{vv}. The values of the impedances K_{hh}, K_{mm} and K_{hm} are defined, for example, in the work of Gazetas.[28] The evaluation of the stiffness K_{vv} is more complicated, since it is related to the vertical deformability of the soil-pile system, which depends on the friction between the lateral surface of the piles and the deformability of the soil under the piles tip. In the commercial software SAP2000 it's possible to define elements with coupled stiffnesses in various degrees of freedom,

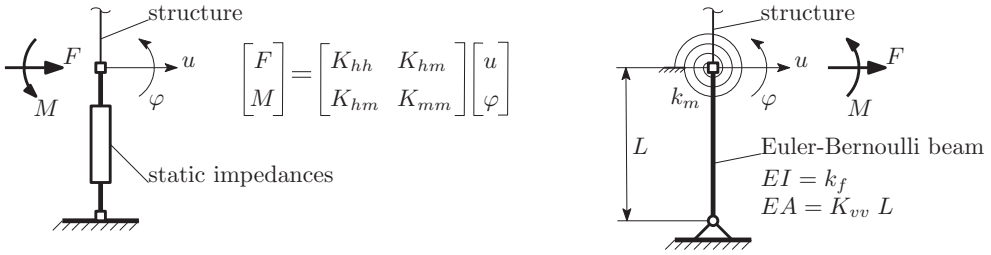

FIGURE A1 Static impedances and equivalent system with Euler-Bernoulli linear beam and a rotational spring.

while in other finite element software, like OpenSees (to date), this is not possible. In Figure A1 an equivalent system that can be used to model static impedances with springs and linear elastic beam elements is outlined.

The system of equations governing this structural scheme is:

$$\begin{bmatrix} F \\ M \end{bmatrix} = \begin{bmatrix} \frac{3k_f}{L^3} & \frac{3k_f}{L^2} \\ \frac{3k_f}{L^2} & \frac{3k_f}{L} + k_m \end{bmatrix} \begin{bmatrix} u \\ \varphi \end{bmatrix} \qquad \text{Parameters:} \begin{cases} k_f = \dfrac{K_{hm}^3}{3K_{hh}^2} \\ k_m = K_{mm} - \dfrac{K_{hm}^2}{K_{hh}} \\ L = \dfrac{K_{hm}}{K_{hh}} \end{cases} \tag{A1}$$

Where k_f is the flexural stiffness of the Euler-Bernoulli beam element, L its length and k_m the stiffness of the rotational spring (see Figure A1). Note that without the rotational spring, the system is ill-conditioned and is characterized by only two parameters instead of three (there must be three parameters to correlate with the three static impedances K_{hh}, K_{mm}, and K_{hm}).